On the existence of flexural edge waves on thin orthotropic plates

Ian Thompson and I. David Abrahams^{a)}

Department of Mathematics, University of Manchester, Oxford Road, Manchester M13 9PL, United Kingdom

Andrew N. Norris

Department of Mechanical and Aerospace Engineering, Rutgers University, Piscataway, New Jersey 08854-8058

(Received 11 January 2002; revised 12 July 2002; accepted 15 July 2002)

This paper is concerned with an investigation into the existence of waves propagating along a free edge of an orthotropic plate, where the edge is inclined at arbitrary angle to a principal direction of the material. After deriving the governing equation and edge conditions, an edge wave ansatz is substituted into this system to reduce it to a set of algebraic equations for the edge wave wave number and wave vector. These are solved numerically for several typical composite materials although analytic expressions can be obtained in the case of special values of the material parameters and inclination angle. It is found that a unique edge wave solution, which generally exhibits oscillation as well as decay away from the free edge, exists in all cases, and its wave speed is independent of its direction of propagation along the plate. © 2002 Acoustical Society of America. [DOI: 10.1121/1.1506686]

PACS numbers: 43.20.Gp, 43.20.Jr, 43.40.Dx [JGH]

I. INTRODUCTION

This paper is concerned with the existence of edge waves propagating on the free edge of a thin elastic plate. Such flexural waves are localized about the edge, i.e., have exponential decay in the direction normal to the free edge, and therefore their energy vector is directed along the edge. These solutions show similarity with other localized waves, such as Rayleigh waves in elasticity, beach waves in water wave theory, etc. The existence of edge waves along the free edge of a homogeneous and isotropic semi-infinite thin plate, modeled using Kirchhoff theory, was first noted by Konenkov¹ in 1960. Published in a Russian journal, this result was little known in the West until it was independently rediscovered by Thurston and McKenna² and by Sinha³ in articles published in 1974. Indeed, it was also "predicted" by De La Rue⁴ in 1972, and surprisingly, continues to this day to be commonly overlooked by researchers (see, e.g., a recent paper by Kauffmann⁵). Konenkov and these other authors established that, for isotropic plates, precisely one edge wave solution exists for all values of the two free parameters, namely the bending stiffness and Poisson's ratio. The edge wave speed is found to be proportional to and slightly less than the speed of flexural (one-dimensional) waves on a plate of infinite extent.

Edge waves are not unique to isotropic Kirchhoff thin plates; Thurston, Boyd, and McKenna⁶ and Krylov⁷ have independently looked for guided elastic modes on the tip of a slender wedge, and work by Norris⁸ in 1994 demonstrated the existence of edge waves in orthotropic Kirchhoff plates. More recently Norris, Krylov, and Abrahams⁹ investigated the propagation of edge waves on thick plates, and did this

theory. Their results were consistent with that found by Konenkov, as were those of Lagasse¹⁰ and Burridge and Sabina, 11,12 who employed finite element modeling to examine the existence of localized waves on the edge of a thick elastic structure employing full three-dimensional elasticity. Experiments in 1976 by Lagasse and Oliner¹³ have demonstrated the existence of the edge wave with wave speed as predicted by theory, although the behavior of the wave speed at higher frequencies is better modeled using the improved theories, such as Mindlin plate theory. 9 Various authors have concerned themselves with the existence of edge waves along fluid-loaded structures: Krylov¹⁴ has an approximate approach to such problems (for plates of wedge shaped cross section submerged in water) employing a ray theory analysis in the limit of high frequency. His results do not prove that such wave can propagate without loss, but there is some experimental support for their existence¹⁵ even if they do radiate a small amount of energy in the direction perpendicular to the edge. Only recent work by Abrahams and Norris¹⁶ has established rigorously that unattenuated edge waves can exist, within a limited frequency window, on thin elastic plates composed of a range of typical materials, from aluminum to PlexiglasTM, submerged in air.

by generalizing the model to incorporate Mindlin plate

The presence or absence of edge waves on thin elastic structures can be of great importance in the field of nondestructive evaluation (NDE) of material components. Ultrasonic elastic waves are regularly employed in NDE to examine an engineering specimen, such as a rotor blade of an aerojet aircraft, and from measurement of the scattered field any imperfections or inclusions in the body can be found. This is an inverse problem, determining the shape, size and *nature* (e.g., inclusion, void, crack, change of phase, etc.) of defects from the overall measured far field. It is helpful, for

a)Electronic mail: i.d.abrahams@ma.man.ac.uk

the development of efficient inverse routines, to have knowledge of forward problems; that is, the scattering signature produced by a wide variety of common material inhomogeneities. For cracks on thin structures this scattering signature can be greatly altered by the existence or nonexistence of flexural edge waves, especially in the shadow zone where the specular field is absent and so the edge wave may be significantly more energetic than the diffracted wave shed from the crack edges. In the context of NDE the authors¹⁷ are currently investigating the forward problem of the diffraction of flexural waves by a semi-infinite crack in a fiber reinforced thin plate, modeled using orthotropic Kirchhoff thin plate theory. This is an important problem to study because of the now widespread use of fiber reinforced and/or laminated materials in industrial applications. These offer extremely strong and light materials but inspection of critical components is still required because of the possibility of delamination, fiber debonding, or other modes of fracture.

For the above-mentioned diffraction problem¹⁷ a crack can, in the general case, be inclined at arbitrary angle to the principal axes of orthotropy. In view of the relevance of edge waves to energy radiation in such models, a precursor study is needed to establish the existence or nonexistence of such waves along inclined edges. Norris⁸ proved existence of a unique edge wave on an orthotropic plate, but this result is only given for the case in which the free edge is parallel to a principal direction of the material. Thus, in this article, the possibility of edge waves in anisotropic Kirchhoff thin plates when the free edge is inclined at general angle to a principal direction is investigated. In Sec. II, the governing equation and edge conditions governing such a system are derived, where the notation employed by Timoshenko and Woinowsky-Krieger¹⁸ is loosely followed. An edge wave ansatz (of the form employed by Konenkov) is substituted into the system, in Sec. III, and from this a set of algebraic equations is obtained for the edge wave wave number and wave vector. These equations are a generalization of those found by Norris, 8 and in general do not permit analytic solutions. For several special values of the material parameters and inclination angle, explicit solutions are readily obtainable and these are discussed in Sec. IV. Finally, numerical solutions to the general system of equations are given in Sec. V, along with some concluding remarks. In particular, it will be shown that a single edge wave solution is found to exist in all cases considered; however, in general, it possesses oscillation as well as decay in the direction orthogonal to the free edge, unlike solutions in previous literature, all of which exhibit pure decay.

II. DERIVATION OF EQUATIONS

The classical equations of plate flexure for an orthotropic, homogeneous thin plate are studied in detail by Timoshenko, ¹⁸ and summarized by Norris. ⁸ Employing the latter author's notation, and taking the principal axes of orthotropy, or fiber direction(s), as x and y, the governing equation for flexural (transverse) displacements W is

$$D_{x}\frac{\partial^{4}W}{\partial x^{4}} + 2H\frac{\partial^{4}W}{\partial x^{2}\partial y^{2}} + D_{y}\frac{\partial^{4}W}{\partial y^{4}} + \rho h\frac{\partial^{2}W}{\partial t^{2}} = 0,$$
 (1)

where ρ is the plate density, h is the plate thickness, t denotes time, and the bending stiffnesses in the x, y directions are D_x , D_y , respectively. Further $H = D_1 + 2D_{xy}$, where D_x , D_y , D_1 , and D_{xy} can be written as

$$D_x = \frac{h^3}{12} \frac{E_1}{1 - \nu_{12}\nu_{21}}, \quad D_y = \frac{\nu_{21}}{\nu_{12}} D_x,$$

$$D_1 = \nu_{21} D_x$$
, $D_{xy} = \frac{h^3}{12} G_{12}$,

and

$$v_{21}E_1 = v_{12}E_2$$
.

Here, the suffixes 1 and 2 refer to the x and y directions, respectively, so E_1 is the Young modulus in the x direction, G_{12} is the shear modulus in the x-y plane, and ν_{12} is the Poisson ratio for transverse strain in the y direction caused by stress in the x direction, with similar definitions for E_2 and ν_{21} . Note that the condition of positive definiteness of strain energy density means that the material parameters must satisfy the following conditions:

$$D_x > 0$$
, $D_y > 0$, $D_{xy} > 0$, $D_x D_y > D_1^2$. (2)

Note that the third inequality gives

$$H>D_1,$$
 (3)

while the final inequality reveals that

$$\sqrt{D_x D_y} > D_1 > -\sqrt{D_x D_y},\tag{4}$$

where D_1 takes negative values when ν_{12} and ν_{21} are negative. It is noted that the bending moments M_x and M_y arising from distributions of in-plane normal stresses σ_x and σ_y , and the twisting moment M_{xy} and shear forces per unit length Q_x , Q_y arising from the shear stresses in the plate, can be written in terms of the transverse displacement, respectively, as

$$M_x = -\left(D_x \frac{\partial^2 W}{\partial x^2} + D_1 \frac{\partial^2 W}{\partial y^2}\right),\tag{5}$$

$$M_{y} = -\left(D_{y}\frac{\partial^{2}W}{\partial y^{2}} + D_{1}\frac{\partial^{2}W}{\partial x^{2}}\right),\tag{6}$$

$$M_{xy} = -M_{yx} = 2D_{xy} \frac{\partial^2 W}{\partial x \partial y},\tag{7}$$

$$Q_x = -\frac{\partial}{\partial x} \left(D_x \frac{\partial^2 W}{\partial x^2} + H \frac{\partial^2 W}{\partial y^2} \right), \tag{8}$$

and

$$Q_{y} = -\frac{\partial}{\partial y} \left(D_{y} \frac{\partial^{2} W}{\partial y^{2}} + H \frac{\partial^{2} W}{\partial x^{2}} \right). \tag{9}$$

As mentioned in Sec. I, a semi-infinite plate is considered where the free-edge is inclined at arbitrary angle to the principal axes of orthotropy. Thus, as shown in Fig. 1, coordinates X, Y are chosen such that the plate is infinite in the X direction, semi-infinite in Y with a free edge along the line Y = 0, and with the principal direction x inclined at an angle $\theta \in [0, \pi/2]$ to the X axis. Expressions are required for the

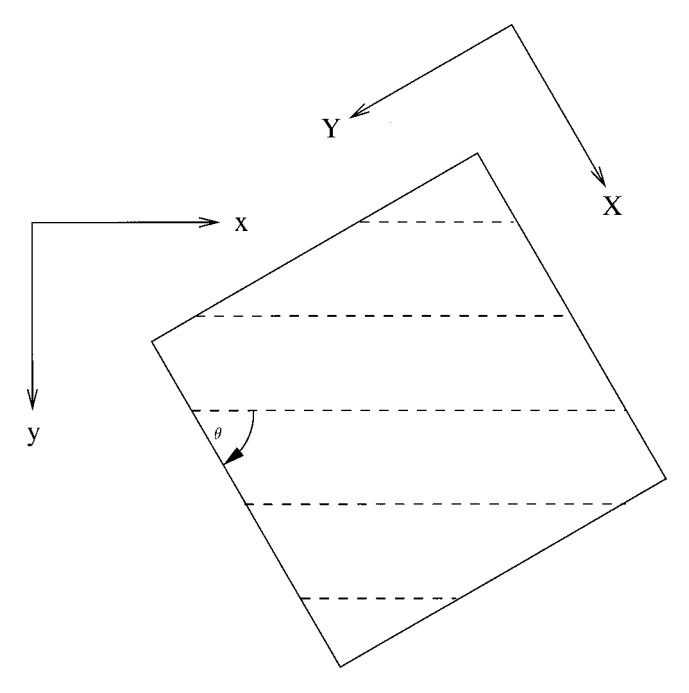


FIG. 1. A square section of the orthotropic plate. The dotted lines represent a principal direction of the material, which is parallel to the x axis, and the free edge lies along Y=0.

bending moment M_Y and the generalized Kirchhoff shear force

$$V_Y = Q_Y + \partial M_{YX} / \partial X, \tag{10}$$

where Q_Y is the shear force arising from the shear stress τ_{YZ} (i.e., acting on the edge at Y=0 but in the direction normal to the plane of the plate) which can be written as

$$Q_{Y} = \frac{\partial M_{Y}}{\partial Y} + \frac{\partial M_{YX}}{\partial X}.$$
 (11)

The free-edge boundary conditions for a Kirchhoff thin plate stipulate that these quantities vanish along this edge (see Graff¹⁹). These conditions can be obtained in terms of the bending and twisting moments in the principal directions x, y by considering a small triangular section of the plate. Omitting details, it is easily shown that

$$M_{Y} = s^{2} M_{x} + c^{2} M_{y} + 2sc M_{xy},$$
 (12)

$$M_{YX} = (s^2 - c^2)M_{xy} - sc(M_x - M_y),$$
 (13)

and also

$$Q_{\gamma} = -sQ_{\chi} + cQ_{\chi}, \tag{14}$$

where here and henceforth the notation $c = \cos \theta$ and $s = \sin \theta$ has been introduced for brevity. Using the coordinate transformation for derivatives,

$$\frac{\partial}{\partial x} = c \frac{\partial}{\partial X} - s \frac{\partial}{\partial Y}, \quad \frac{\partial}{\partial y} = s \frac{\partial}{\partial X} + c \frac{\partial}{\partial Y},$$

with Eqs. (1), (5)–(9), (10), (11), and (12)–(14), the entire system is now rewritten in terms of derivatives parallel and perpendicular to the edge of the plate. Thus, the governing equation becomes

$$\left[D_{x}\left(s\frac{\partial}{\partial Y}-c\frac{\partial}{\partial X}\right)^{4}+2H\left(s\frac{\partial}{\partial Y}-c\frac{\partial}{\partial X}\right)^{2}\left(c\frac{\partial}{\partial Y}+s\frac{\partial}{\partial X}\right)^{2}\right] + D_{y}\left(c\frac{\partial}{\partial Y}+s\frac{\partial}{\partial X}\right)^{4}W+\rho h\frac{\partial^{2}W}{\partial t^{2}}=0, \tag{15}$$

while the bending moment is given by

$$\begin{split} M_{Y} &= -\left[(s^{2}D_{x} + c^{2}D_{1}) \left(c \frac{\partial}{\partial X} - s \frac{\partial}{\partial Y} \right)^{2} + (s^{2}D_{1} + c^{2}D_{y}) \right. \\ &\times \left(c \frac{\partial}{\partial Y} + s \frac{\partial}{\partial X} \right)^{2} + 4scD_{xy} \left(s \frac{\partial}{\partial Y} - c \frac{\partial}{\partial X} \right) \\ &\times \left(c \frac{\partial}{\partial Y} + s \frac{\partial}{\partial X} \right) \right] W, \end{split} \tag{16}$$

and the Kirchhoff generalized shear force is

$$V_{Y} = \left\{ s \left[-H \left(s \frac{\partial}{\partial Y} - c \frac{\partial}{\partial X} \right) \left(c \frac{\partial}{\partial Y} + s \frac{\partial}{\partial X} \right)^{2} - D_{x} \left(s \frac{\partial}{\partial Y} - c \frac{\partial}{\partial Y} \right)^{2} \right. \\ \left. - c \frac{\partial}{\partial X} \right)^{3} \right] + c \left[-H \left(s \frac{\partial}{\partial Y} - c \frac{\partial}{\partial X} \right)^{2} \left(c \frac{\partial}{\partial Y} + s \frac{\partial}{\partial X} \right) \right. \\ \left. - D_{y} \left(c \frac{\partial}{\partial Y} + s \frac{\partial}{\partial X} \right)^{3} \right] - \frac{\partial}{\partial X} \left[s c (D_{1} - D_{x}) \right. \\ \left. \times \left(s \frac{\partial}{\partial Y} - c \frac{\partial}{\partial X} \right)^{2} + s c (D_{y} - D_{1}) \left(c \frac{\partial}{\partial Y} + s \frac{\partial}{\partial X} \right)^{2} \right. \\ \left. + 2 (s^{2} - c^{2}) D_{xy} \left(s \frac{\partial}{\partial Y} - c \frac{\partial}{\partial X} \right) \left(c \frac{\partial}{\partial Y} + s \frac{\partial}{\partial X} \right) \right] \right\} W.$$

$$(17)$$

III. EDGE WAVE SOLUTIONS

Following the approach of Konenkov, ¹ a solution of the governing equation (1) is sought, of the form

$$W = \Re[(A_1 e^{-\gamma_1 k_0 Y} + A_2 e^{-\gamma_2 k_0 Y}) e^{i(\xi k_0 X - \omega t)}], \tag{18}$$

where ω is the frequency and k_0 is a suitable wave number selected so that the parameter ξ lies in the range $(1,\infty)$. For exponential decay away from the free edge, the coefficients γ_1 and γ_2 must lie in the open right half plane. This represents a flexural edge wave solution, i.e., where the energy is confined to the vicinity of Y=0, propagating in the positive X direction. Clearly, for a comprehensive study of the existence of such waves, the case of propagation in the -X direction must also be examined. For convenience this is most neatly incorporated by maintaining $\xi \in (1,\infty)$ and instead without loss of generality allowing the orientation angle θ to range over $[-\pi/2,\pi/2]$ (Fig. 1). This symmetry is easily observed by changing $\sin(\theta)$ to $\sin(-\theta)$, and $\partial/\partial X$ to $-\partial/\partial X$, in (15)-(17); the governing equation and boundary conditions remain unaltered.

To simplify the subsequent analysis, it is convenient to write

$$\gamma_i = -i\,\xi\lambda_i\,,\tag{19}$$

for $j \in \{1,2\}$, and thus both λ_1 and λ_2 must lie in the open upper half plane. The edge wave now becomes

$$W = (A_1 e^{i\xi k_0 \lambda_1 Y} + A_2 e^{i\xi k_0 \lambda_2 Y}) e^{i(\xi k_0 X - \omega t)}$$
(20)

and substitution into Eq. (15) yields the auxiliary equations:

$$D_x(s\lambda_j-c)^4+2H(s\lambda_j-c)^2(c\lambda_j+s)^2+D_y(c\lambda_j+s)^4$$

$$-\frac{R}{\xi^4} = 0, \quad j \in \{1, 2\},\tag{21}$$

where

$$R = \frac{\rho h \omega^2}{k_0^4} \,. \tag{22}$$

This is a quartic polynomial in λ , with real coefficients, which can be rewritten in the form

$$a_1 \lambda^4 + b_1 \lambda^3 + a_2 \lambda^2 + b_2 \lambda + \left(a_3 - \frac{R}{\xi^4} \right) = 0,$$
 (23)

with

$$a_1 = s^4 D_x + c^4 D_y + 2s^2 c^2 H,$$
 (24)

$$b_1 = 4sc[-s^2D_x + c^2D_y + H(s^2 - c^2)],$$
 (25)

$$a_2 = 6s^2c^2(D_x + D_y - 2H) + 2H,$$
 (26)

$$b_2 = 4sc[-c^2D_x + s^2D_y - H(s^2 - c^2)], \tag{27}$$

$$a_3 = c^4 D_x + s^4 D_y + 2s^2 c^2 H. (28)$$

As stated, the edge wave must decay as $Y \rightarrow \infty$ and so the two roots λ_1 and λ_2 must have positive imaginary parts; the two remaining roots of (23) are therefore their complex conjugates λ_1^* and λ_2^* . Hence (29) may be cast as

$$a_1(\lambda - \lambda_1)(\lambda - \lambda_1^*)(\lambda - \lambda_2)(\lambda - \lambda_2^*) = 0 \tag{29}$$

from which it can be deduced that the constant term is

$$a_3 - \frac{R}{\xi^4} = a_1 |\lambda_1|^2 |\lambda_2|^2. \tag{30}$$

Now, the inequalities in (3), (4) can be employed to show that

$$a_{1} = s^{4}D_{x} + c^{4}D_{y} + 2s^{2}c^{2}H > s^{4}D_{x} + c^{4}D_{y} + 2s^{2}c^{2}2D_{1} >$$

$$s^{4}D_{x} + c^{4}D_{y} - 2s^{2}c^{2}\sqrt{D_{x}D_{y}} = (s^{2}\sqrt{D_{x}} - c^{2}\sqrt{D_{y}})^{2} \ge 0$$
(31)

and similarly

$$a_3 > (c^2 \sqrt{D_x} - s^2 \sqrt{D_y})^2 \ge 0$$
 (32)

for *all* values of the parameters. Therefore, the right-hand side of (30) is greater than zero and rearranging gives the bound

$$\xi^4 > \frac{R}{a_3}.\tag{33}$$

It is thus convenient to choose k_0 so that

$$R = a_3 = c^4 D_x + s^4 D_y + 2s^2 c^2 H, (34)$$

thereby ensuring that $\xi \in (1,\infty)$. Note that this particular value of k_0 is the wave number of a plane wave traveling in the X direction, and the positivity of the normalized wave phase

speed $1/\xi$ is a direct consequence of the positivity of the strain energy in the plate.

Now, on using Eqs. (16) and (17), and applying the boundary conditions $M_Y=0$ and $V_Y=0$ along the line Y=0, it can be shown that

$$\sum_{j=1}^{2} A_{j} [D_{x}s^{2}(s\lambda_{j}-c)^{2} + D_{y}c^{2}(c\lambda_{j}+s)^{2} + 2Hsc(s\lambda_{j}-c)(c\lambda_{j}+s) + D_{1}] = 0,$$
(35)

and

$$\sum_{j=1}^{2} A_{j} [D_{x} s(s\lambda_{j} - c)^{2} (s\lambda_{j} - 2c) + D_{y} c(c\lambda_{j} + s)^{2} (c\lambda_{j} + 2s) + 2H(s\lambda_{j} - c)(c\lambda_{j} + s)(sc\lambda_{j} + s^{2} - c^{2}) - D_{1}\lambda_{j}] = 0.$$
(26)

The unknown quantities A_1 and A_2 can be then eliminated between these last two equations to give the dispersion relation:

$$\mathcal{F}(\lambda_1, \lambda_2) = \mathcal{F}(\lambda_2, \lambda_1) \tag{37}$$

in which

$$\mathcal{F}(\lambda_{1},\lambda_{2}) = [D_{x}s^{2}(s\lambda_{1}-c)^{2} + D_{y}c^{2}(c\lambda_{1}+s)^{2} + 2Hsc(s\lambda_{1}-c)(c\lambda_{1}+s) + D_{1}]$$

$$\times [D_{x}s(s\lambda_{2}-c)^{2}(s\lambda_{2}-2c) + D_{y}c(c\lambda_{2}+s)^{2}$$

$$\times (c\lambda_{2}+2s) + 2H(s\lambda_{2}-c)(c\lambda_{2}+s)$$

$$\times (sc\lambda_{2}+s^{2}-c^{2}) - D_{1}\lambda_{2}]. \tag{38}$$

The roots, λ_j , j=1,2 of the polynomial (21) can be substituted into (38) so that it is a single equation for the wave number ξ . In the cases treated in earlier literature, both γ_1 and γ_2 were found to be positive real. This corresponds to positive imaginary values of λ_1 and λ_2 , but is impossible in general, since setting $\lambda = iL$, with $L \in \mathbb{R}^+$, and taking the imaginary part of Eq. (21) yields

$$sc[D_{x}s^{2}-D_{y}c^{2}+H(c^{2}-s^{2})]L^{2}$$

$$=sc[D_{x}c^{2}-D_{y}s^{2}-H(c^{2}-s^{2})],$$
(39)

from which it is clear that two distinct real positive values of L cannot exist except in cases where both sides of this equation are zero, which are discussed in the following section. In general, therefore, edge waves must exhibit oscillation as well as decay in the Y direction, and Eq. (37) must be solved numerically; this is performed in Sec. V.

At the beginning of this section the angle of orientation, θ , between the free edge Y=0 and the principal direction of orthotropy y=0 was taken over $[-\pi/2,\pi/2]$ in order to account for all possible edge wave solutions. It is now convenient to relate the form of the edge wave for negative values of θ (or left traveling waves) to that for positive θ (right traveling waves) and thereby restrict attention henceforth, without loss of generality, to $\theta \in [0,\pi/2]$. If the angle θ is replaced by $-\theta$ in the auxiliary equation (23) then the coefficients a_j , j=1,2,3 remain the same while b_1 and b_2 change their signs. Therefore, the four roots are related to the

TABLE I. Coefficient values in each of the special cases.

Case	a_1	a_2	a_3	b
i	D	2D	D	D_1
ii	D_{v}	2H	D_x	D_1
iii	D_x	2H	D_{v}	D_1
iv	(H+D)/2	3D-H	(H+D)/2	$(D-H)/2+D_1$

former roots; these are now $-\lambda_1^*$, $-\lambda_2^*$ in the upper half plane and $-\lambda_1$, $-\lambda_2$ in the lower half plane. From this it can be concluded that the change of sign of the orientation angle yields a change in sign in the real part of λ_j , j = 1,2, while the imaginary part (the decay rate in the Y direction) remains the same. With the changed λ_j the dispersion relation (37) becomes

$$\mathcal{F}(-\lambda_1^*, -\lambda_2^*)\big|_{\theta \to -\theta} = \mathcal{F}(-\lambda_2^*, -\lambda_1^*)\big|_{\theta \to -\theta},\tag{40}$$

where \mathcal{F} is given in Eq. (38). This is just the conjugate equation to Eq. (37) and so yields the same real root ξ , if one exists. In conclusion, left and right propagating edge waves have the same phase speed, and decay with identical exponents in the direction Y perpendicular to the edge. However, inspection of Eqs. (35) and (36) reveals that A_j , j=1,2 are changed to their complex conjugates as θ changes sign, and for left traveling waves the oscillatory behavior in Y for each of the two exponents in W (20) is exactly out of phase with that for right traveling waves.

IV. SPECIAL CASES

As well as allowing the possibility of real values of γ_1 and γ_2 , the vanishing of both sides of Eq. (39) gives rise to four special cases in which an analytical solution is easily obtained. It is noted that, in view of the inequalities (2), the terms of Eq. (23) which are of order zero, two, and four in λ are strictly positive; hence meaningful simplification occurs only when the coefficients of λ^3 and λ , b_1 and b_2 , are simultaneously zero. By inspection of Eq. (39), it is evident that there are four cases to consider, namely:

- (i) $D_x = D_y = H = D$ (say);
- (ii) $\theta = 0$;
- (iii) $\theta = \pi/2$;
- (iv) $D_x = D_y = D$ (say), $\theta = \pi/4$.

Of the above, (i) is that of isotropy, as investigated by Konenkov,¹ Thurston and McKenna,² etc., (ii) and (iii) are essentially equivalent and were discussed by Norris,⁸ and (iv) appears to be new. In each case, Eq. (23) is reduced to the form

$$a_1 \lambda_j^4 + a_2 \lambda_j^2 + a_3 \left(1 - \frac{1}{\xi^4} \right) = 0,$$
 (41)

and the dispersion relation (37) becomes

$$\lambda_2[a_1\lambda_1^2+b][a_1\lambda_2^2+(a_2-b)]$$

$$= \lambda_1 [a_1 \lambda_2^2 + b][a_1 \lambda_1^2 + (a_2 - b)]. \tag{42}$$

For each of the above-mentioned cases, the values of a_1 , a_2 , a_3 , and b are given in Table I. It is important to

note that, in each case, due to the inequalities (2), the following relations hold:

$$a_1 > 0$$
, $a_3 > 0$, $a_2 - 2b > 0$, $a_1 a_3 > b^2$. (43)

An example of case (iv) could be, for instance, a fiber reinforced plate with identical fibers aligned in both x and y directions. Clearly, $\theta = \pm \pi/4$ are also lines of symmetry, and so the plate can be viewed as orthotropic with principal axes X and Y when $\theta = \pi/4$. From Table I it is seen that, in this rotated frame, the effective H value is $a_2/2 = (3D - H)$ and the bending stiffnesses $(a_1 \text{ and } a_3)$ are $D_X = D_Y = (H + D)/2$.

Equation (41) may be solved to give the values of λ_1 and λ_2 in terms of the as yet unknown parameter ξ . Thus,

$$\lambda_{j}^{2} = \frac{1}{2a_{1}} \left[-a_{2} + (-1)^{j} \left[a_{2}^{2} - 4a_{1}a_{3} \left(1 - \frac{1}{\xi^{4}} \right) \right]^{1/2} \right], \quad (44)$$

which immediately yields the relations

$$\lambda_1^2 + \lambda_2^2 = -\frac{a_2}{a_1},\tag{45}$$

and

$$\lambda_1^2 \lambda_2^2 = \frac{a_3}{a_1} \left(1 - \frac{1}{\xi^4} \right). \tag{46}$$

Now, since λ_1 and λ_2 must lie in the upper half plane, it follows that either λ_1^2 and λ_2^2 are real and negative, or [by Eq. (44)], they are complex conjugates. In either case, we have

$$\lambda_1^2 = re^{i\phi},$$

for some positive r and $\phi \in [-\pi,0)$. Again using the fact that λ_1 and λ_2 must lie in the upper half plane, this leads to

$$\lambda_1 = \sqrt{r}e^{i(\phi/2 + \pi)},$$

and

$$\lambda_2 = \sqrt{r}e^{-i\phi/2}.$$

Consequently, it is clear from (46) that

$$\lambda_1 \lambda_2 = -\sqrt{a_3/a_1} \sqrt{1 - 1/\xi^4}. \tag{47}$$

In view of this, along with Eq. (45), the dispersion relation (42) reduces to

$$a_1 a_3 \left(1 - \frac{1}{\xi^4}\right) + \sqrt{a_1 a_3} (a_2 - 2b) \sqrt{1 - \frac{1}{\xi^4}} - b^2 = 0.$$
 (48)

Possible roots for ξ are now easily obtained; factoring the quadratic in (48) yields

$$\sqrt{1 - \frac{1}{\xi^4}} = \frac{-(a_2 - 2b) \pm \sqrt{(a_2 - 2b)^2 + 4b^2}}{2\sqrt{a_1 a_3}},$$

and since the left-hand side is positive, we must choose the "+" sign to obtain a solution. Thus, the unique root for ξ is the positive value which satisfies

$$\frac{1}{\xi^4} = 1 - \frac{1}{4a_1a_3} [(a_2 - 2b) - \sqrt{(a_2 - 2b)^2 + 4b^2}]^2.$$
 (49)

TABLE II. Material parameters (modulii units are GPa).

Reinforcing fibers	E_1	E_2	ν_{12}	G_{12}
Glass	54.2	18.1	0.250	8.96
Boron	208	20.8	0.300	6.95
Graphite	208	5.21	0.250	2.59
Bidirectional glass	54.2	54.2	0.250	8.96

Finally, note that a necessary and sufficient condition for pure imaginary values of λ_1 and λ_2 in these cases is obtained by substituting (49) into Eq. (44); the resulting inequality is

$$(a_2-2b)[-a_2+6b+2\sqrt{(a_2-2b)^2+4b^2}]>0.$$

Using the fact that $a_2 > 2b$, it is straightforward to show that λ_1 and λ_2 lie at distinct points on the imaginary axis provided that

$$a_2 > -\frac{2}{3}b$$
, (50)

otherwise the solution will exhibit oscillation away from the free edge. Note that, since a_2 is greater than 2b, the inequality (50) can only be violated if b is negative. In addition, a repeated root may arise (i.e., $\lambda_1 = \lambda_2$; this occurs when

$$a_2 = -\frac{2}{3}b. (51)$$

In this case, it can be expected that a solution of the form

$$W = (A_1 + A_2 Y) e^{-\gamma_1 k_0 Y} e^{i(\xi X k_0 - \omega t)}$$

holds instead of the standard edge wave ansatz (18). It is important to note, however, that in general the parameters required to satisfy Eq. (51) will not occur.

V. NUMERICAL SOLUTIONS AND CONCLUDING REMARKS

Numerical solutions of Eq. (21) and (37) were obtained by using a linear search to locate an interval in which the function

$$f(\xi) = \mathcal{F}(\lambda_1, \lambda_2) - \mathcal{F}(\lambda_2, \lambda_1),$$

possesses a zero. The bisector algorithm was then employed to find a value of ξ for which

$$|f(\xi)| < 10^{-12}$$
.

This was carried out for four sets of parameters, representing epoxy resin plates with a variety of reinforcing fibers (see Table II). The first three sets of data are taken from Norris, and the fourth is included to illustrate special case (iv) discussed in Sec. IV. In each example, precisely one value of ξ was found in the interval $(1,\infty)$; these results are shown in Fig. 2. The ordinate of this figure is $1/\xi$, which is the edge wave phase speed normalized with respect to the wave speed of flexural waves propagating along the X direction, i.e., ω/k_0 . Note the proximity of the solutions to $\xi=1$ when $\theta\approx0$, $\pi/2$, and also that the plot for bidirectional glass is symmetric about $\theta=\pi/4$ as expected since $D_x=D_y$ here. To reveal the *absolute* magnitudes of the wave speeds as θ varies, Fig. 2 is replotted for the nondimensional propagation speed c_n in the various media (Fig. 3), where

$$c_n = \left(\frac{R}{D_x}\right)^{1/4} \frac{1}{\xi} = \frac{\omega^{1/2}}{k_0 \xi} \left(\frac{\rho h}{D_x}\right)^{1/4},$$

i.e., this is the phase speed relative to that for a plane flexural wave traveling in the x direction. As one might intuitively expect, the magnitude in the change of c_n with angle of inclination appears to be directly related to the value of $|E_1 - E_2|$ (and, consequently $|D_x - D_y|$), with materials exhibiting stronger orthotropy experiencing greater changes in phase speed. Thus, for graphite fibers, with E_1/E_2 around 40, c_n varies from unity to less than 0.4 as θ increases to $\pi/2$.

Values of γ_1 and γ_2 associated with Figs. 2 and 3 were also computed; all three plates with unidirectional fiber support exhibited similar behavior in this respect. Plots of the real and imaginary part of γ_1 and γ_2 for boron fibers are shown in Figs. 4 and 5. The real parts of both γ_1 and γ_2

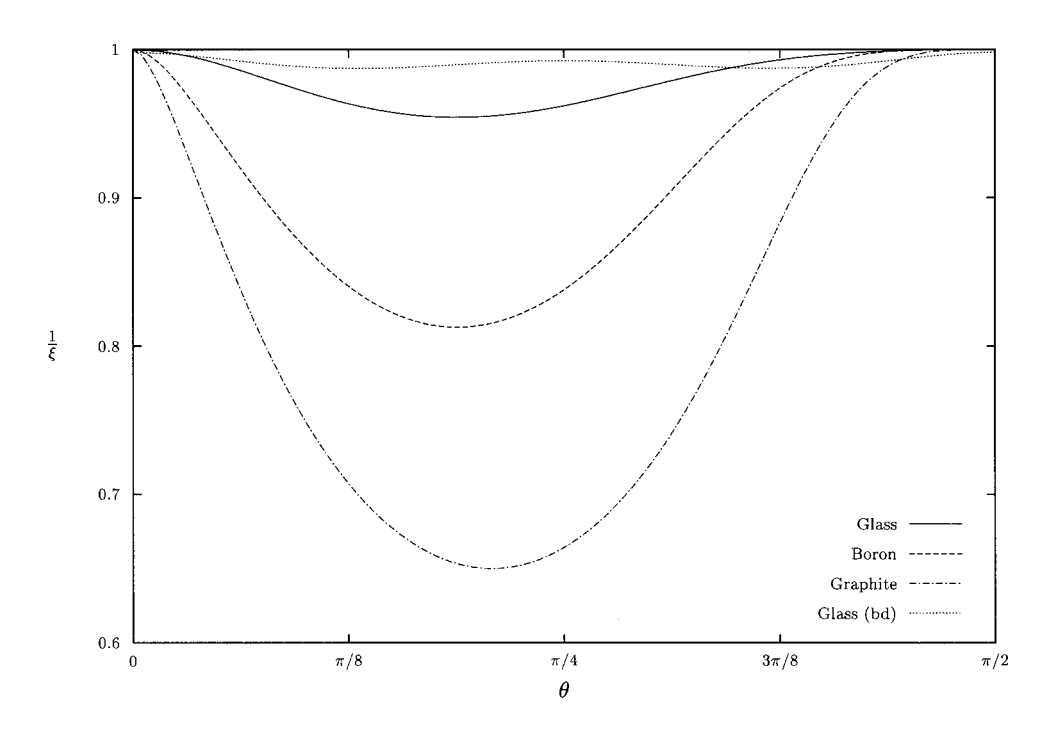


FIG. 2. Phase speed of edge waves in the respective media normalized with respect to flexural waves propagating in the *X* direction, i.e., parallel to the plate edge.

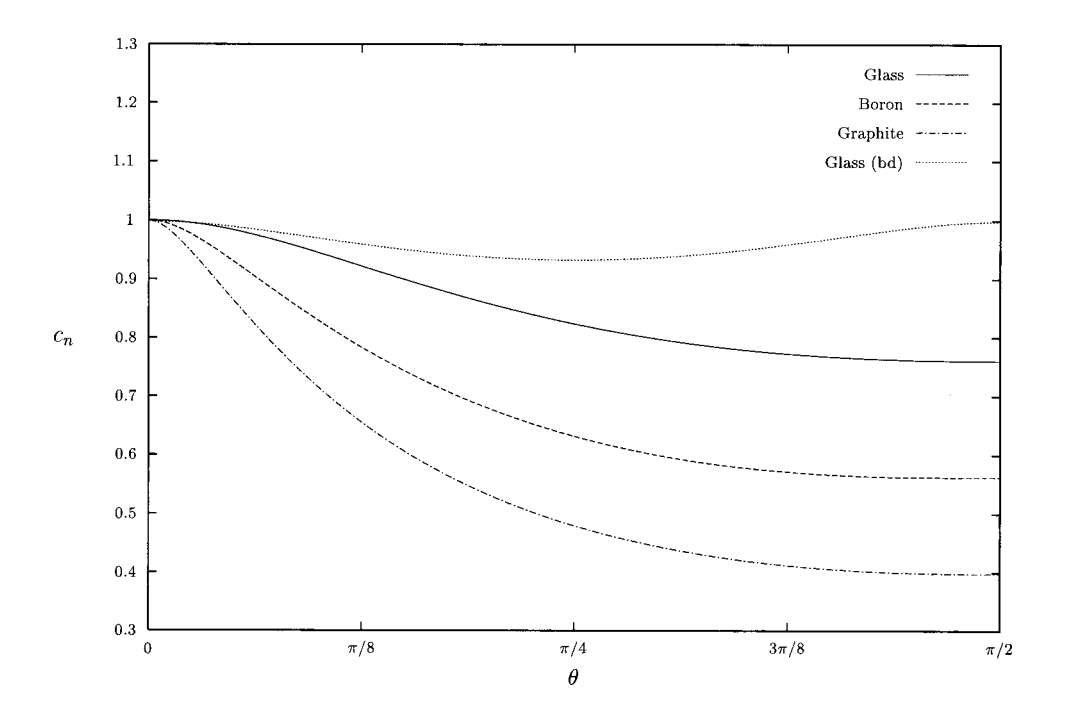


FIG. 3. Phase speed of edge waves in the respective media normalized with respect to flexural waves propagating in the principal *x* direction.

show a clear maximum, indicating the point of strongest decay for their respective exponent term in W (18), though the maxima do not occur at quite the same angle of inclination. Note also that the occurrences of $\Im(\gamma_1) = \Im(\gamma_2) = 0$ agree with the results of Sec. IV. Different behavior was observed in the values of γ_1 and γ_2 for bidirectional glass fibers, Figs. 6 and 7, as might be expected. Here, the curves are symmetric about $\theta = \pi/4$, and both $\Re(\gamma_1)$ and $\Re(\gamma_2)$ exhibit maxima at this angle. In this case, $\Im(\gamma_1) = \Im(\gamma_2) = 0$ for $\theta \in \{0, \pi/4, \pi/2\}$, again agreeing with the results of Sec. IV. In all cases, the weakest decay is observed at the limit values $\theta = 0$ and $\theta = \pi/2$, since the curves for $\Re(\gamma_1)$ and $\Re(\gamma_2)$ both exhibit minima here. This is to be expected, since, when $\theta \approx 0$, $\pi/2$, the wave number is close to $\xi = 1$, i.e., the value for straight crested flexural waves.

Further understanding of the oscillatory behavior associ-

ated with complex values of γ_1 and γ_2 can be gained by considering the flexural displacement with nondimensional arguments, defined as

$$\hat{W} = \Re \left\{ (A_1 + A_2) \sum_{j=1}^{2} \left(\frac{A_j}{A_1 + A_2} \right) \exp[-\gamma_j (D_x / R)^{1/4} \hat{Y}] \right. \\
\times \exp[i\xi (D_x / R)^{1/4} \hat{X} - i\omega t] \right\}.$$
(52)

Here, the spatial coordinates have been normalized with respect to the wave number of flexural waves in the *x* direction, i.e.,

$$\hat{X} = \left(\frac{\rho h \omega^2}{D_x}\right)^{1/4} X,$$

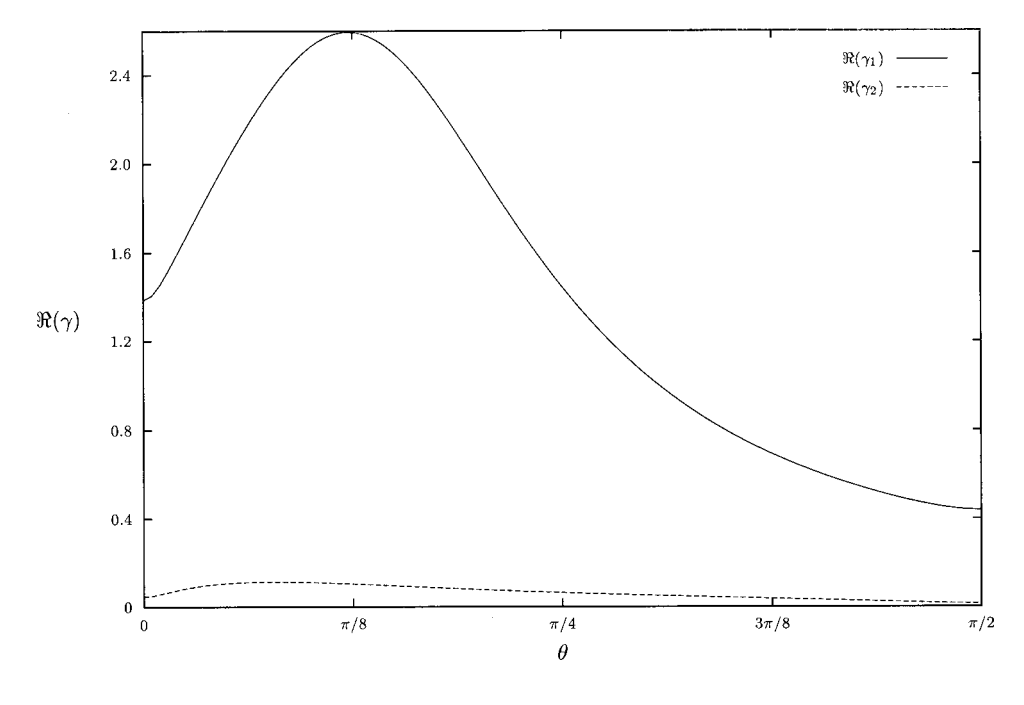


FIG. 4. Values of the decay coefficients $\Re(\gamma_j)$ for boron/epoxy.

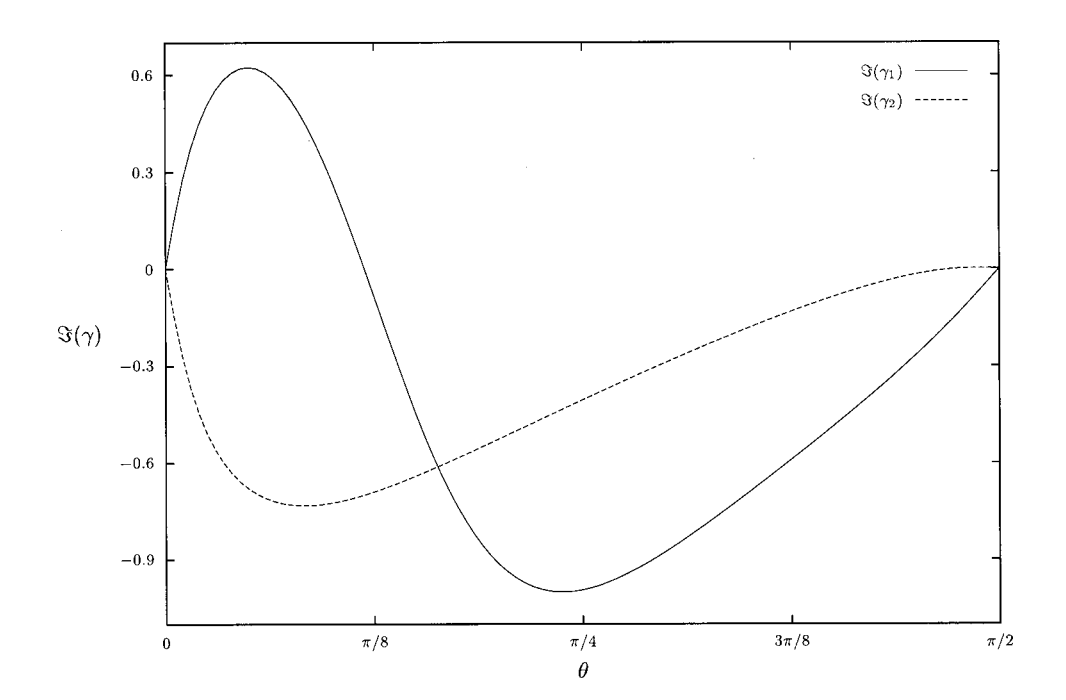


FIG. 5. Values of the oscillation coefficients $\Im(\gamma_j)$ for boron/epoxy.

and

$$\hat{Y} = \left(\frac{\rho h \omega^2}{D_x}\right)^{1/4} Y.$$

A contour plot of the function \hat{W} can then be produced, for a given value of the (arbitrary) constant $A_1 + A_2$ and for any fixed time. This consists (see Fig. 8) of a regular pattern of lobes of alternating sign, separated by "null" lines on which $\hat{W}=0$. In all of these cases investigated herein it is found that $\Re(\gamma_1) \gg \Re(\gamma_2)$ (also $A_1/A_2 < 0.3$), so the behavior of the wave is almost completely determined by the relative sizes of $\Re(\gamma_2)$ and $\Im(\gamma_2)$, i.e.,

$$\hat{W} \approx \Re\{A_2 \exp[(D_x/R)^{1/4}(i\xi\hat{X} - \gamma_2\hat{Y}) - i\omega t]\}.$$

By explicitly separating real and imaginary parts, it is easy to show that an accurate estimate for the angle of deviation, ϕ ,

of the null lines from the direction normal to the free edge, \hat{Y} , is given by

$$\phi \approx \arctan\left(-\frac{\Im(\gamma_2)}{\xi}\right)$$

where ϕ is measured positive counterclockwise looking down onto the plate as in Fig. 8. Thus in the limit cases θ =0 and θ = π /2, the null lines are perpendicular to the edge, since $\Im(\gamma_2)$ =0 here. In general the null lines are inclined to the edge, though one should note that despite efforts by the authors no obvious relation between ϕ and the principal directions could be ascertained. This is borne out by a plot of ϕ against the inclination angle θ given in Fig. 9. For the materials with unidirectional fiber support, ϕ >0, since $\Im(\gamma_2)$ <<0, so the null lines tilt away from the direction of propagation. For bidirectional glass fiber support, however, ϕ >0

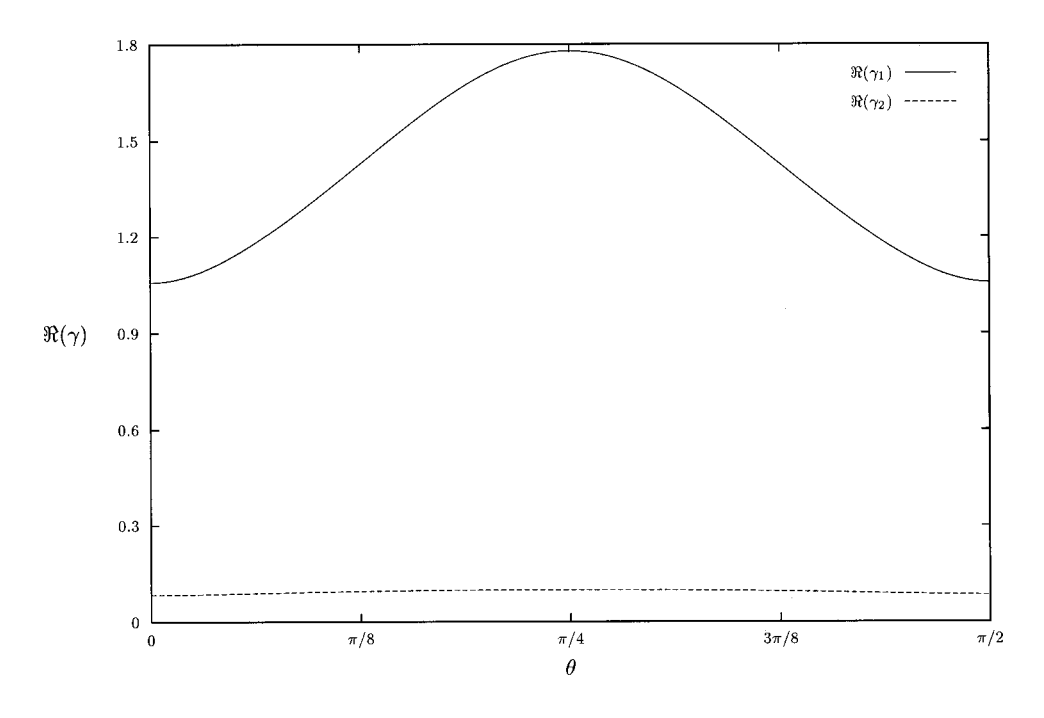


FIG. 6. Values of the decay coefficients $\Re(\gamma_j)$ for bidirectional glass/epoxy.

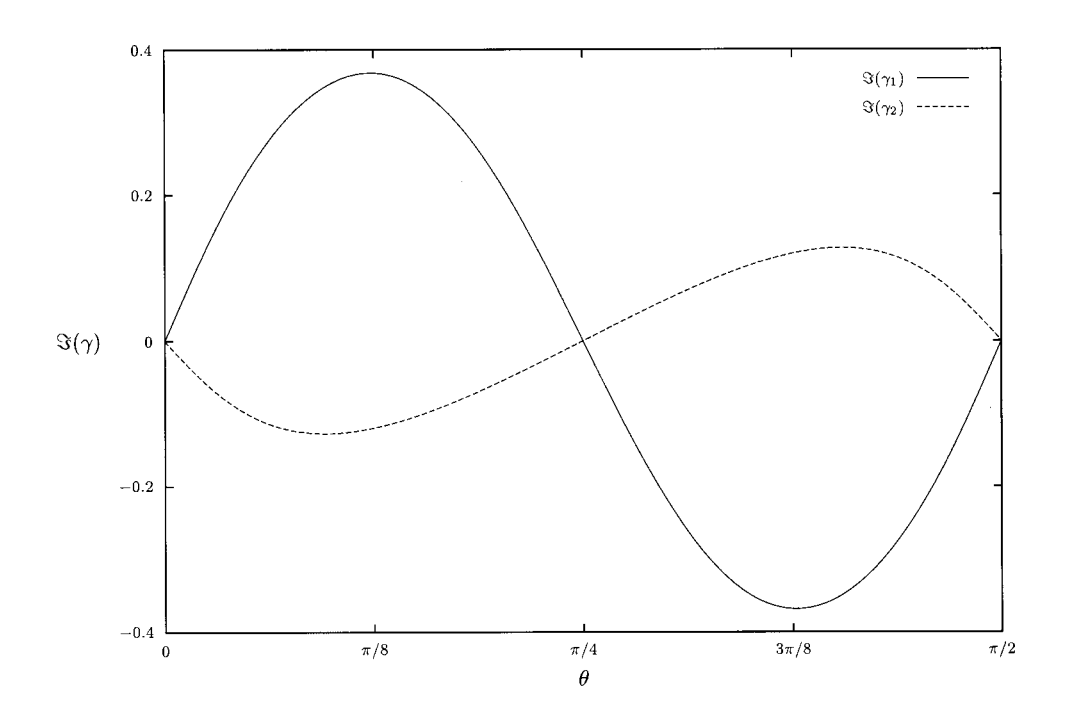


FIG. 7. Values of the oscillation coefficients $\Im(\gamma_j)$ for bidirectional glass/epoxy.

for $0 < \phi < \pi/4$, and $\phi < 0$ for $\pi/4 < \theta < \pi/2$. Due to the inclination of the null lines, a straight line perpendicular to the edge (in the \hat{Y} direction) will pass alternately through regions in which \hat{W} is positive and negative, thereby giving rise to the oscillations shown in earlier figures.

To summarize, numerical evidence suggests that, as for

the special cases discussed in Sec. IV and in previous literature, in general a unique edge wave solution exists for every set of material parameters and inclination angle. The wave generally exhibits both oscillation and decay away from the free edge; the oscillation arising due to the "tilting" of the solution pattern which occurs when $\theta \in (0, \pi/2)$ (see Figs. 8

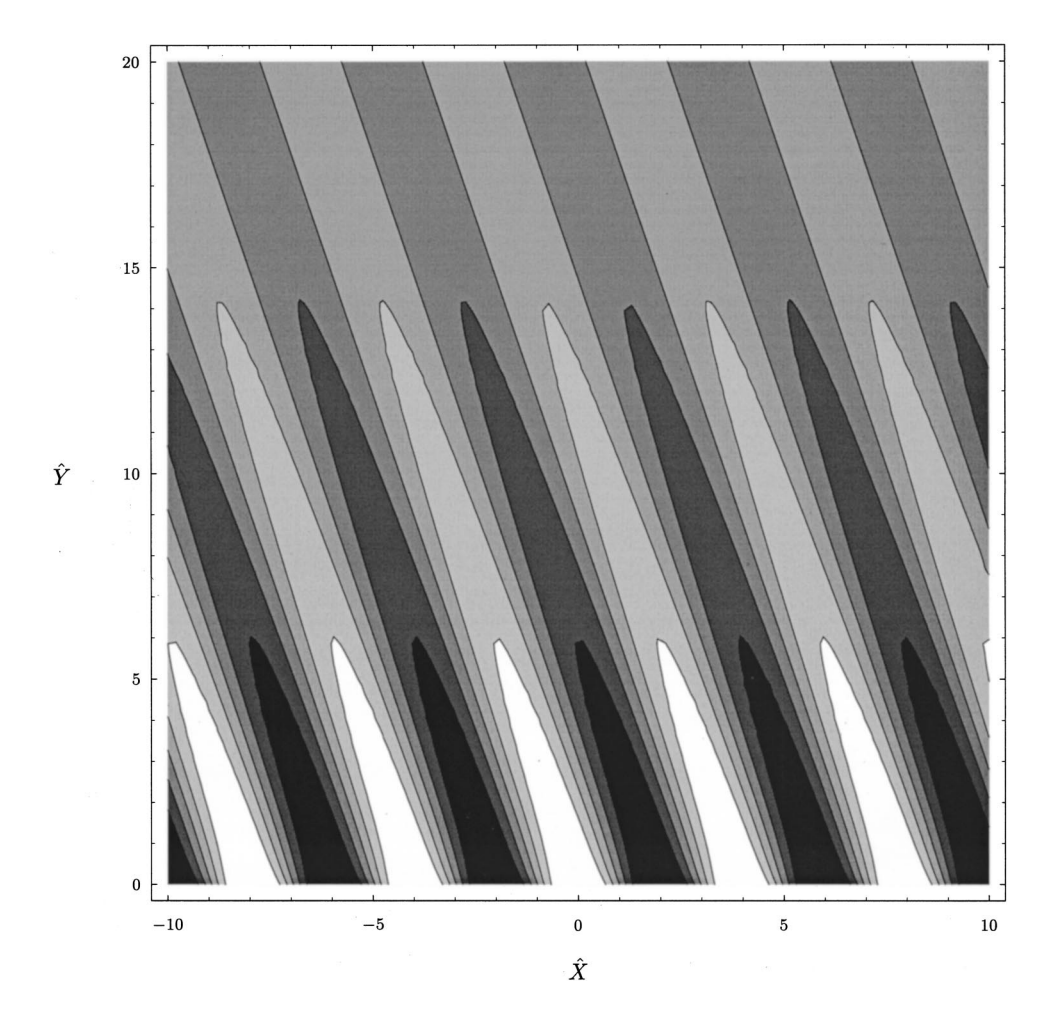


FIG. 8. Contour plot of the nondimensional flexural displacement \hat{W} at time $t\!=\!0$, for boron/epoxy in the case $\theta\!=\!\pi/4$, with $A_1\!+\!A_2\!=\!1$. Positive values of \hat{W} occur in regions with lighter shading; dark shading indicates \hat{W} $<\!0$.

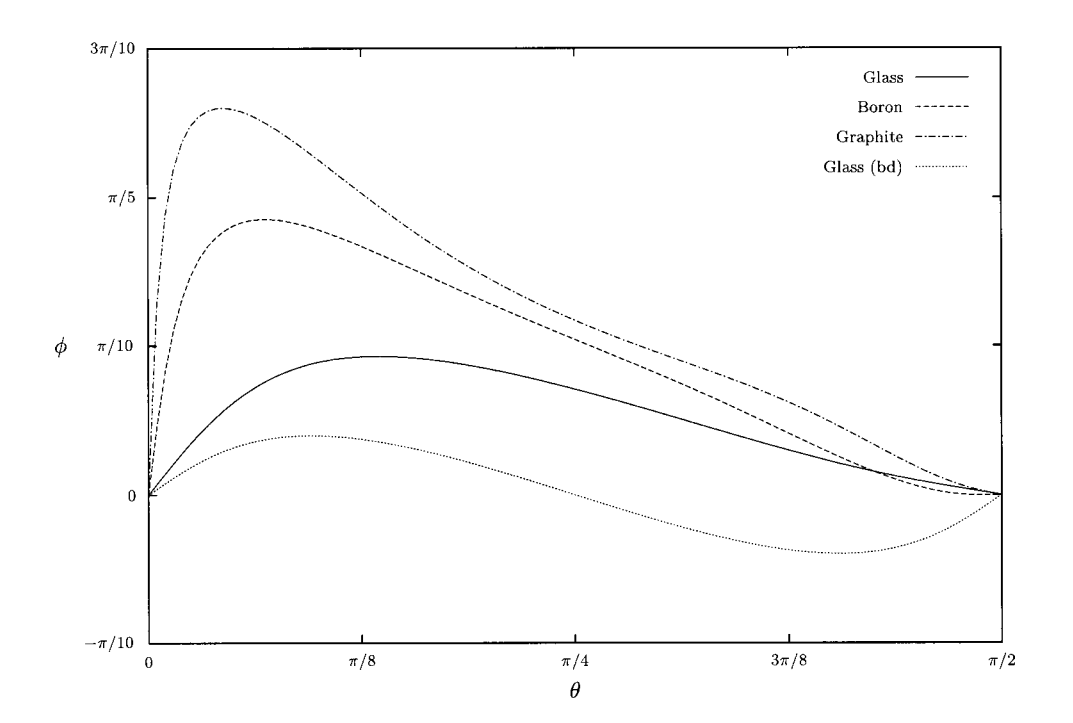


FIG. 9. Deviation angle ϕ of the null lines from the direction normal to the free edge (measured positive counterclockwise).

and 9 and the discussion in the preceding paragraph). Edge waves propagating in the negative X direction travel with the same speed as their counterparts with phase vector pointing in the positive X direction; however, their oscillatory behavior in the orthogonal direction Y is π out of phase. That is, in Eq. (18), when X is changed to -X, the complex conjugate of the expression in parentheses is taken. A final important point to note concerns the values of the parameters for which edge waves have pure decay in the Y direction. Norris's previous article8 might lead a reader to hold the mistaken impression that, for θ =0, π /2 [i.e., cases (ii) and (iii) of Sec. IV], all parameter values will lead to $\Im(\gamma_i) = 0$, j = 1,2. This is not true, and by inspection of his Eq. (7), or equivalently (45), γ_j , j = 1,2, certainly cannot be positive real when H (or a_2) is less than or equal to zero. However, there are also positive values of H for which the Y behavior is oscillatory. This can be deduced from the inequality (50), which, from Table I, implies that pure decay away from the edge occurs if and only if

$$H > -\frac{D_1}{3} \tag{53}$$

or equivalently

$$D_{xy} > -\frac{2D_1}{3},$$
 (54)

and so for $D_1 < 0$ this yields a window of positive values of H and D_{xy} for which this condition is violated.

ACKNOWLEDGMENTS

The authors are grateful to the Engineering and Physical Sciences Research Council, UK for the support of a research studentship for Thompson and to the Leverhulme Trust, UK, for a *Grant in Aid of Research* for Abrahams.

- ¹Yu. K. Konenkov, "A Rayleigh-type flexural wave," Sov. Phys. Acoust. 6, 122–123 (1960).
- ² R. N. Thurston and J. McKenna, "Flexural acoustic waves along the edge of a plate," IEEE Trans. Sonics Ultrason. 21, 296–297 (1974).
- ³B. K. Sinha, "Some remarks on propagation characteristics of ridge guides for acoustic waves at low frequencies," J. Acoust. Soc. Am. 56, 16–18 (1974).
- ⁴R. M. De La Rue, "Experimental and theoretical studies of guided acoustic surface wave propagation," Ph.D. thesis, University College, London, 1972.
- ⁵C. Kauffmann, "A new bending wave solution for the classical plate equation," J. Acoust. Soc. Am. **104**, 2220–2222 (1998).
- ⁶R. N. Thurston, G. D. Boyd, and J. McKenna, "Plate theory solution for guided flexural acoustic waves along the tip of a wedge," IEEE Trans. Sonics Ultrason. 21, 178–186 (1974).
- ⁷ V. V. Krylov, "Geometrical-acoustics approach to the description of localized modes of an elastic solid wedge," Sov. Phys. Tech. Phys. **35**, 137–140 (1990).
- A. N. Norris, "Flexural edge waves," J. Sound Vib. 171, 571–573 (1994).
 A. N. Norris, V. V. Krylov, and I. D. Abrahams, "Flexural edge waves and comments on 'a new bending wave solution for the classical plate equation," J. Acoust. Soc. Am. 107, 1781–1784 (2000).
- ¹⁰P. E. Lagasse, "Higher-order finite-element analysis of topographic guides supporting elastic surface waves," J. Acoust. Soc. Am. **53**, 1116–1122 (1973).
- ¹¹ R. Burridge and F. J. Sabina, "Theoretical computations on ridge acoustic surface waves using the finite element method," Electron. Lett. 7, 720– 722 (1971).
- ¹²R. Burridge and F. J. Sabina, "The propagation of elastic surface waves guided by ridges," Proc. R. Soc. London, Ser. A 330, 417–441 (1972).
- ¹³ P. E. Lagasse and A. A. Oliner, "Acoustic flexural mode on a ridge of semi-infinite height," Electron. Lett. 12, 11–13 (1976).
- ¹⁴ V. V. Krylov, "On the velocities of localized vibration modes in immersed solid wedges," J. Acoust. Soc. Am. **103**, 767–770 (1998).
- ¹⁵ M. de Billy, "On the influence of loading on the velocity of guided elastic waves in linear elastic wedges," J. Acoust. Soc. Am. **100**, 659–662 (1996).
- ¹⁶ I. D. Abrahams and A. N. Norris, "On the existence of flexural edge waves on submerged elastic plates," Proc. R. Soc. London, Ser. A 456, 1559–1582 (2000).
- ¹⁷I. Thompson and I. D. Abrahams, "Diffraction of flexural waves by a semi-infinite crack in a fibre reinforced thin elastic plate" (unpublished).
- ¹⁸S. Timoshenko and S. Woinowsky-Krieger, *Theory of Plates and Shells*, 2nd ed. (McGraw-Hill, New York, 1959).
- ¹⁹ K. F. Graff, Wave Motion in Elastic Solids (Dover, New York, 1991).